

TECHNICAL
PHYSICS

Suppression of Impulsive Noise in Multichannel Images Using Fuzzy Logics and the Angular Divergence of Pixels

V. F. Kravchenko^{a*}, V. I. Ponomaryov^{b**}, and Academician V. I. Pustovoit^c

Received June 25, 2008

PACS numbers: 07.05.Mh, 07.05.Pj

DOI: 10.1134/S1028335808110074

1. Based on the ideas described in [1–6], we substantiate and propose an approach to attain a method of impulsive-noise suppression. This approach makes it possible to reconstruct image contours and image fine details. For comparison with the method proposed, other well-known algorithms were analyzed. We imply the AMNF and AMNF2 filters [3], and also the AMNF3 [5, 10] and the GVDF [6] filters that employ the angular-divergence technique in the multichannel pixels, as well as the WVDF1, WVDF2, LWVDF, CWVDF, and SWVDF algorithms [7, 8]. The latter algorithms are based on geodesic trajectories. The PVMM [9] and VMF SAR [10] filters constructed on the basis of the highest statistics theory were also used.

The approach proposed in the present study makes use of the method of pixel angular divergence in a multichannel image together with the theory of fuzzy sets, which forms the filtered final image.

2. The method developed allows us to determine the presence of noise, contours, and fine details in a sliding window in the course of image processing. The processing is realized in the 3×3 sliding window, where 8 pixels (from x_0 to x_7) neighboring the central pixel x_c are employed. The color-image pixel at the point i is considered as the vector x_i with three components, namely, red (R), green (G), and blue (B): $x_i = (x_i^R, x_i^G, x_i^B)$. The sliding 3×3 window is inside a large 5×5 window used for the determination of quantities in different directions with respect to neighboring pixels in the 3×3 processing window.

The eight pixels neighboring the central pixel x_c each correspond to one direction, namely, N (north), E

(east), S (south), and W (west), NW (northwest), NE (northeast), SE (southeast), and SW (southwest), as is shown in Fig. 1.

We now define gradients in the form $\nabla x_k^R = |x_c^R - x_k^R|$, $\nabla x_k^G = |x_c^G - x_k^G|$, $\nabla x_k^B = |x_c^B - x_k^B|$, $k = 0, 1, \dots, n^2 - 2$ and repeatedly denote them with allowance for Fig. 1. Thus, we obtain

$$\begin{aligned} & \nabla[x_c^\beta(i, j), x^\beta(i+k, j+l)] \\ &= |x_c^\beta(i, j) - x^\beta(i+k, j+l)| = \nabla_{(k,l)}^\beta x(i, j), \quad (1) \\ & k, l \in (-1, 0, +1), \quad \beta = (R, G, B). \end{aligned}$$

Here, each of the pairs (k, l) corresponds to one of eight pixel directions at the point (i, j) . Eight values of the gradient associated with the corresponding directions are called basic gradient values (see Fig. 1). In order to avoid spreading contours and fine details, we use four auxiliary gradient quantities. They are calculated with respect to the basic gradient. The calculation procedure for the SE direction is clarified in Fig. 1. For this direc-

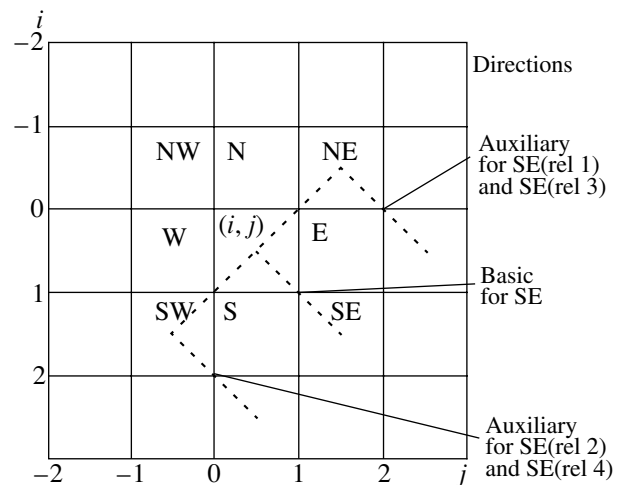


Fig. 1. Basic and auxiliary directions for gradients and vector quantities (SE).

^a Institute of Radio Engineering and Electronics, Russian Academy of Sciences, Moscow, 103907 Russia

^b National Polytechnic Institute, 04430 Mexico City, Mexico

^c Scientific and Technological Center of Unique Instrumentation, Russian Academy of Sciences, Moscow, 117342 Russia

e-mail: *kyf@pochta.ru; **vponomar@mail.ru

tion, the basic gradient is $\nabla_{(1,1)}^\beta x(i, j) = \nabla_{SE}^\beta$, whereas four auxiliary gradients are written out as

$$\begin{aligned} \nabla_{(0,2)}^\beta x(i-1, j+1) &= \nabla_{SE(rel1)}^\beta, \\ \nabla_{(2,0)}^\beta x(i+1, j-1) &= \nabla_{SE(rel2)}^\beta, \quad \nabla_{(i,j)}^\beta x(i-1, j+1) = \\ \nabla_{SE(rel3)}^\beta, \quad \nabla_{(i,j)}^\beta x(i+1, j-1) &= \nabla_{SE(rel4)}^\beta. \end{aligned}$$

Introducing the subscript $\gamma = (N, E, S, W, NW, NE, SE, SW)$, we determine the gradient values for the case of the basic direction and its four complementary values in the case of other directions similarly to the case of the SE direction. We now introduce two fuzzy sets called SMALL and BIG. The SMALL set determines the level of the membership function for the gradient quantity in the case when its value is sufficiently small and the membership function takes a large value. Thus, when the value of the membership function is close to unity, this guarantees the absence of movement (no-movement case) and/or the absence of noise (no-noise case) in the sampling to be analyzed. In other case, when gradient quantities exhibit significant differences between their components, this determines large values of the membership function in the BIG fuzzy set. The Gaussian membership functions used in these cases are written out as

$$\mu(\nabla_\gamma^\beta \text{SMALL}) = \begin{cases} 1, & \text{if } \nabla_\gamma^\beta < \text{med}_2, \\ \exp\left\{-\frac{(\nabla_\gamma^\beta - \text{med}_2)^2}{2\sigma_1^2}\right\} & \text{otherwise,} \end{cases} \quad (2)$$

$\text{med}_2 = 10, \sigma_1^2 = 1000$; and

$$\mu(\nabla_\gamma^\beta \text{BIG}) = \begin{cases} 1, & \text{if } \nabla_\gamma^\beta > \text{med}_1, \\ \exp\left\{-\frac{(\nabla_\gamma^\beta - \text{med}_1)^2}{2\sigma_1^2}\right\} & \text{otherwise,} \end{cases} \quad (3)$$

$\text{med}_1 = 60$.

We now determine the angular deviation between multichannel vectors $x_1 = (x_1^R, x_1^G, x_1^B)$ and $x_2 = (x_2^R, x_2^G, x_2^B)$ for each component (color). For example, for the R component in the SE direction, we write out the basic angular deviation and four auxiliary angular deviations in the form

$$\begin{aligned} \theta_{(1,1)}^R x(i, j) &= \theta_{SE}^R, \quad \theta_{(0,2)}^R x(i-1, j+1) = \theta_{SE(rel1)}^R, \\ \theta_{(2,0)}^R x(i+1, j-1) &= \theta_{SE(rel2)}^R, \\ \theta_{(i,j)}^R x(i-1, j+1) &= \theta_{SE(rel3)}^R, \\ \theta_{(i,j)}^R x(i+1, j-1) &= \theta_{SE(rel4)}^R. \end{aligned}$$

Fuzzy values of angular deviations are characterized by the Gaussian membership function

$$\mu(\theta_\gamma^\beta \text{SMALL}) = \begin{cases} 1, & \text{if } \theta_\gamma^\beta < \text{med}_3, \\ \exp\left\{-\frac{(\theta_\gamma^\beta - \text{med}_3)^2}{2\sigma_2^2}\right\} & \text{otherwise,} \end{cases} \quad (4)$$

$\text{med}_3 = 0.8, \sigma_2^2 = 0.8$; and

$$\begin{aligned} \mu(\theta_\gamma^\beta \text{BIG}) \\ = \begin{cases} 1, & \text{if } \theta_\gamma^\beta > \text{med}_4, \\ \exp\left\{-\frac{(\theta_\gamma^\beta - \text{med}_4)^2}{2\sigma_2^2}\right\} & \text{otherwise,} \end{cases} \end{aligned} \quad (5)$$

$\text{med}_4 = 0.1$.

The proposed fuzzy rules are based on gradient quantities and angular deviations. They are used to determine the fact whether the central pixel corresponds to noise and/or to the absence of noise, or if this is a local movement.

Fuzzy rule 1 determines the value of the fuzzy angular and gradient quantity $\nabla_\gamma^{\beta F} \theta_\gamma^{\beta F}$:

IF (∇_γ^β is BIG AND $\nabla_{\gamma(rel1)}^\beta$ is SMALL AND $\nabla_{\gamma(rel2)}^\beta$ is SMALL AND $\nabla_{\gamma(rel3)}^\beta$ is BIG AND $\nabla_{\gamma(rel4)}^\beta$ is BIG) AND (θ_γ^β is BIG AND $\theta_{\gamma(rel1)}^\beta$ is SMALL AND $\theta_{\gamma(rel2)}^\beta$ is SMALL AND $\theta_{\gamma(rel3)}^\beta$ is BIG AND $\theta_{\gamma(rel4)}^\beta$ is BIG)

THEN $\nabla_\gamma^{\beta F} \theta_\gamma^{\beta F}$ is BIG.

This fuzzy rule contains nine conjunctions. The operators being used in the fuzzy conjunction are defined for two cases: (1) outside of the brackets, the AND operator is equivalent to $\min(A; B)$, (2) inside the brackets, it is defined as $A \text{ AND } B = A \cap B$. The membership function for the central pixel $x_c^\beta(i, j)$ in the BIG fuzzy set and in the γ direction is defined as $\nabla_\gamma^{\beta F} \theta_\gamma^{\beta F}$ and is calculated in the following manner:

$$\begin{aligned} \nabla_\gamma^{\beta F} \theta_\gamma^{\beta F} &= \min(\mu(\nabla_\gamma^\beta \text{BIG}) \cdot \mu(\nabla_{\gamma(rel1)}^\beta \text{SMALL}) \\ &\times \mu(\nabla_{\gamma(rel2)}^\beta \text{SMALL}) \cdot \mu(\nabla_{\gamma(rel3)}^\beta \text{BIG}) \cdot \mu(\nabla_{\gamma(rel4)}^\beta \text{BIG}); \\ &\mu(\theta_\gamma^\beta \text{BIG}) \cdot \mu(\theta_{\gamma(rel1)}^\beta \text{SMALL}) \cdot \mu(\theta_{\gamma(rel2)}^\beta \text{SMALL}) \\ &\times \mu(\theta_{\gamma(rel3)}^\beta \text{BIG}) \cdot \mu(\theta_{\gamma(rel4)}^\beta \text{BIG})). \end{aligned} \quad (6)$$

The multichannel central pixel is considered to be a noise pixel or belongs to the BIG fuzzy set when the basic quantities $\mu(\nabla_\gamma^\beta)$ and $\mu(\theta_\gamma^\beta)$ are close to their aux-

iliary quantities $(\mu(\nabla_{\gamma(\text{rel}3)}^\beta), \mu(\nabla_{\gamma(\text{rel}4)}^\beta), (\mu(\theta_{\gamma(\text{rel}3)}^\beta), \mu(\theta_{\gamma(\text{rel}4)}^\beta))$ and also differ from the quantities $(\mu(\nabla_{\gamma(\text{rel}1)}^\beta), \mu(\nabla_{\gamma(\text{rel}2)}^\beta), (\mu(\theta_{\gamma(\text{rel}1)}^\beta), \mu(\theta_{\gamma(\text{rel}2)}^\beta))$. The presence of noise is determined with the help of the following fuzzy rule.

Fuzzy rule 2 determines for an fuzzy quantity the value of the noise factor in the form r^β :

IF $\nabla_N^{\beta F} \theta_N^{\beta F}$ is BIG OR $\nabla_S^{\beta F} \theta_S^{\beta F}$ is BIG OR $\nabla_E^{\beta F} \theta_E^{\beta F}$ is BIG OR $\nabla_W^{\beta F} \theta_W^{\beta F}$ is BIG OR $\nabla_{SW}^{\beta F} \theta_{SW}^{\beta F}$ is BIG OR $\nabla_{NE}^{\beta F} \theta_{NE}^{\beta F}$ is BIG OR $\nabla_{NW}^{\beta F} \theta_{NW}^{\beta F}$ is BIG OR $\nabla_{SE}^{\beta F} \theta_{SE}^{\beta F}$ is BIG THEN r^β is BIG.

According to this rule, large values of the membership function in the BIG (noise) fuzzy set testify to the presence of noise in the sampling, which is used in the algorithm for noise suppression. This also determines the type of filtration in dependence on the fact whether this is a noise pixel or this is a local variation of the image. Fuzzy rule 2 contains seven disjunctions, and the operator being used for the disjunctions is defined as

$$r^\beta = \max(\nabla_{SE}^{\beta F} \theta_{SE}^{\beta F}, \max(\nabla_{NW}^{\beta F} \theta_{NW}^{\beta F}, \max(\nabla_{NE}^{\beta F} \theta_{NE}^{\beta F}, \max(\nabla_{SW}^{\beta F} \theta_{SW}^{\beta F}, \max(\nabla_W^{\beta F} \theta_W^{\beta F}, \max(\nabla_E^{\beta F} \theta_E^{\beta F}, \max(\nabla_N^{\beta F} \theta_N^{\beta F}, \nabla_S^{\beta F} \theta_S^{\beta F})))))))). \quad (7)$$

3. The value of the membership function for the central pixel is determined in the fuzzy noise set. Here, we use the following rule to determine whether a pixel corresponds to the noise component or is noise-free. IF $r^\beta \geq 0.3$ THEN the filtration is realized on the basis of the values of the membership function being determined for the BIG fuzzy set. Otherwise, the filter is determined as not varied pixel $y_{\text{output}}^\beta = x_c^\beta$.

The threshold value 0.3 is determined on the basis of optimum values for criteria in the course of processing simulation according to the given algorithm. Insofar as the values of the membership function yield the weights for each component, we make use of the negation operator. For the membership function of the noise-free NO BIG fuzzy set, this operator is written out in the form $\xi_\gamma^{\beta F} = 1 - \nabla_\gamma^{\beta F} \theta_\gamma^{\beta F}$. For the central pixel,

the weight was chosen as $\xi_c^{\beta F} = 3\sqrt{1-r^\beta}$. The values of the components in the 3×3 sampling window are $x_\gamma^\beta = (x_{SW}^\beta, x_S^\beta, x_{SE}^\beta, x_W^\beta, x_c^\beta, x_E^\beta, x_{NW}^\beta, x_N^\beta, x_{NE}^\beta)$. They are presented in increasing order and determine the

ordering for the corresponding weights of the fuzzy logics:

$$\begin{aligned} x_\gamma^{\beta(1)} \leq x_\gamma^{\beta(2)} \leq x_\gamma^{\beta(3)} \leq x_\gamma^{\beta(4)} \leq x_\gamma^{\beta(5)} \leq x_\gamma^{\beta(6)} \leq x_\gamma^{\beta(7)} \\ \leq x_\gamma^{\beta(8)} \leq x_\gamma^{\beta(9)} \Rightarrow \xi_\gamma^{\beta(1)} \leq \xi_\gamma^{\beta(2)} \leq \xi_\gamma^{\beta(3)} \leq \xi_\gamma^{\beta(4)} \\ \leq \xi_\gamma^{\beta(5)} \leq \xi_\gamma^{\beta(6)} \leq \xi_\gamma^{\beta(7)} \leq \xi_\gamma^{\beta(8)} \leq \xi_\gamma^{\beta(9)}. \end{aligned} \quad (8)$$

The filtration procedure results in the choice of one of the neighboring components possessing the least probability to be distorted by noise. It was proposed to realize the filtration using not only weights of the fuzzy logics but also their ordering, which is seen from formula (8). This allows us to exclude the components located at a sufficiently long distance with respect to the central pixel. This is realized by introducing the variable $\text{sum}^\beta = \xi_\gamma^{\beta(j)}$, where j decreases from 9 to 1, the decrease of j being correct as long as

$$\text{sum}^\beta > \frac{\sum \xi_\gamma^{\beta F} + 3\sqrt{1-r^\beta}}{2}.$$

We also define the variable $\text{sum}^\beta = \xi_\gamma^{\beta(j)}$, where j varies from 9 to 3 as long as this condition is satisfied. We find the output value for the filter as the j_{th} ordered value for the number j satisfying the inequality

$$\text{sum}^\beta > \frac{\sum \xi_\gamma^{\beta F} + 3\sqrt{1-r^\beta}}{2}.$$

If the condition for $j \leq 2$ is not fulfilled, then we choose for the j_{th} ordered value the output one: $y_{\text{output}}^\beta = x_\gamma^{\beta(j)}$.

4. The properties of the filter proposed and of algorithms well known in the literature were studied on the basis of standard criteria, namely, the *peak signal-to-noise ratio* expressed in decibels (PSNR) [4-6], *mean absolute error* (MAE) [7], and *the normalized chromatic difference* (NCD) [10, 11]. 320×320 pixel color test images (Lena, Baboon, Peppers, Parrots, and Goldhill) (RGB-space, 24 bits) were independently distorted by impulsive noise of various intensities in each image channel. Among other algorithms that had been studied by us, there were ABST_* and Wilc_ [3], MAMNFE, AMNF, AMNF2 [3], AMNF [4, 11], AVMF [10], SAPFRWA- [12], BVDF- and GVDF-filters [3], the INR algorithm [2], the WVDF1, WVDF2, LWVDF, CWVDF, and SWVDF filters [7], the MMKNN*-* filters [4, 5, 10], the PVMM algorithm [8], and the VMF SAR filter [12].

Table 1 shows the testing results for the best filters among the aforementioned ones. This table confirms that the novel algorithm is the best under conditions of both low-intensity and intermediate-intensity noise (from 0 to 30%). Table 2 illustrates values of the PSNR criterion for the *Baboon* test image. The proposed

Table 1. NCD values for *Lena* color image (noise 0–50%)

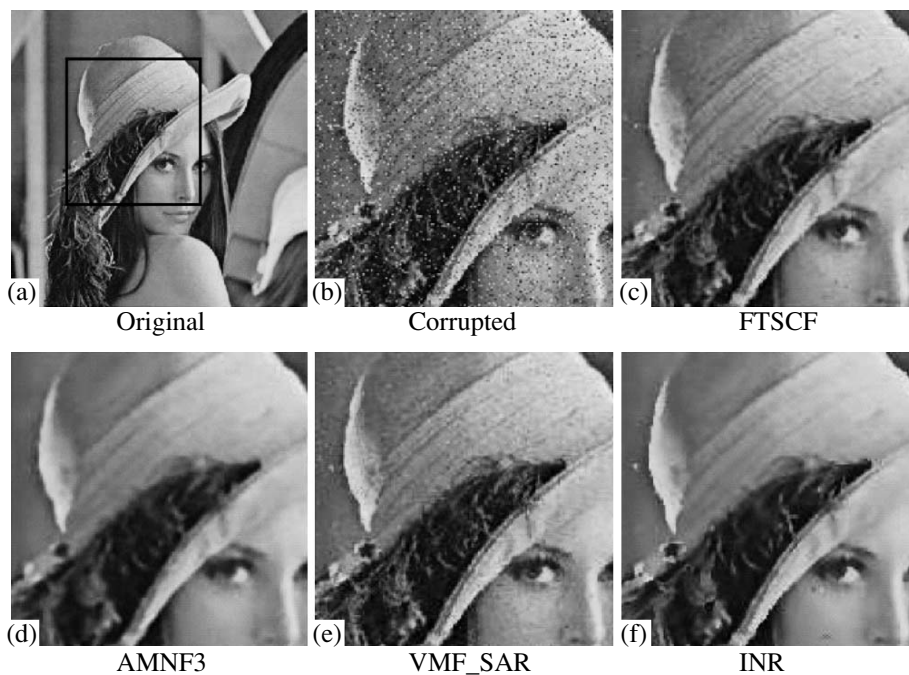
Filter	0	5	10	15	20	25	30	40	50
ABST_CMS	0.0195	0.203	0.213	0.0226	0.024	0.0258	0.0283	0.0359	0.0465
AMNF2	0.019	0.0199	0.0207	0.0217	0.0228	0.0244	0.0264	0.0338	0.0453
AMNF3	0.0188	0.0195	0.0203	0.0212	0.0222	0.0234	0.0252	0.0316	0.0418
VMF	0.0154	0.0162	0.0171	0.0185	0.02	0.0221	0.0252	0.0348	0.0485
FDCF	0.0017	0.0037	0.0059	0.0084	0.0115	0.0158	0.0206	0.0352	0.0537
INR	0.0164	0.0166	0.0171	0.0176	0.0184	0.0197	0.0214	0.0281	0.0405
LWVDF	0.017	0.0187	0.0208	0.0234	0.0265	0.0307	0.0362	0.0524	0.0744
MMKNN_CMS	0.0159	0.0168	0.0178	0.0191	0.0206	0.0225	0.0251	0.0333	0.0452
VMF_SAR	0.001	0.0044	0.0085	0.0134	0.0178	0.0228	0.0278	0.0415	0.0585
Wilc_CMS	0.0073	0.0096	0.0128	0.0166	0.0207	0.0255	0.0302	0.0434	0.0592
WVDF1	0.0137	0.0156	0.0181	0.0213	0.025	0.0302	0.0367	0.0544	0.0766

Table 2. Results obtained according to PSNR criterion for *Baboon* color image (noise 0–50%)

Filter	0	3	5	10	15	20	30	40	50
AMNF3	23.84	23–75	23.65	23.57	23.44	23.41	23.34	23.15	21.35
FDCF	29.24	28.31	27.41	27.16	26.82	25.32	23.25	18.83	15.75
INR	27.32	26.93	26.64	26.51	26.47	25.83	24.82	22.83	19.85
VMF_SAR	30.12	28.32	27.32	26.41	24.84	23.34	22.45	18.65	17.74

FDCF algorithm operates efficiently in correspondence with the PSNR criterion within the noise-intensity range from 3 to 15%. The MAE criterion shows that the novel filter is the best within the noise-inten-

sity range from 7 to 35%. Figure 2 presents the zoomed *Lena* image demonstrating the best reconstruction of contours and fine details compared to well-known filters.

**Fig. 2.** Zoomed image (“Lena”) distorted by impulsive noise of 15% intensity.

5. Thus, the approach developed and realized in the novel FDCF filter uses combined processing based on the angular information and the theory of fuzzy sets. This algorithm has shown its high efficiency in the suppression of impulsive noise and in reconstruction of contours and details, as well as chromatic characteristics. This is in correspondence with both widely used PSNR, MAE, and NCD criteria and visual estimates of filtered images.

REFERENCES

1. V. F. Kravchenko, V. I. Ponomaryov, and V. I. Pustovoit, Dokl. Phys. **53**, 363 (2008) [Dokl. Akad. Nauk **421**, 190 (2008)].
2. S. Schulte, S. Morillas, V. Gregori, and E. Kerre, IEEE Trans. Image Process. **16**, 2565 (2007).
3. K. N. Plataniotis, D. Androustos, S. Vinayagamoorthy, and A. N. Venetsanopoulos, IEEE Trans. Image Process. **6**, 933 (1997).
4. V. F. Kravchenko, V. I. Ponomaryov, V. I. Pustovoit, and R. Samores-Pech, Dokl. Phys. **51**, 304 (2006) [Dokl. Akad. Nauk **408**, 469 (2006)].
5. V. I. Ponomaryov, F. J. Gallegos-Funes, and A. Rosales-Silva, J. Imaging Sci. Technol. **49**, 205 (2005).
6. P. E. Trahanias and A. N. Venetsanopoulos, IEEE Trans. Image Process. **2**, 528 (1993).
7. R. Lukac, B. Smolka, K. N. Plataniotis, and A. N. Venetsanopoulos, Comput. Vis. Image Underst. **94**, 140 (2004).
8. M. Szczepanski, B. Smolka, K. N. Plataniotis, and A. N. Venetsanopoulos, Signal Process. **83**, 1309 (2003).
9. N. Alajlan, M. Kamel, and E. Jernigan, Signal Process. Image Commun. **19**, 993 (2004).
10. B. Smolka, R. Lukac, A. Chydzinski, et al., Real-Time Imag. **9**, 261 (2003).
11. V. Ponomaryov, J. Real-Time Image Process. **1**, 173 (2007).
12. R. Lukac, Pattern. Recogn. Lett. **24**, 1889 (2003).

Translated by G. Merzon